International Journal of Pharmaceutics 358 (2008) 60–68

Contents lists available at ScienceDirect

International Journal of Pharmaceutics

journal homepage: www.elsevier.com/locate/ijpharm

Relationship between dissolution efficiency of Oxazepam/carrier blends and drug and carrier molecular descriptors using multivariate regression analysis

Annalisa Cutrignelli[a], Angela Lopedota[a], Adriana Trapani[a], Giancarlo Boghetich[a,b], Massimo Franco[a], Nunzio Denora[a], Valentino Laquintana[a], Giuseppe Trapani[a,*]

[a] *Dipartimento Farmaco-Chimico, Facoltà di Farmacia, Università degli Studi di Bari, Via Orabona 4, 70125 Bari, Italy*
[b] *Dipartimento di Ingegneria Civile ed Ambientale I Facoltà di Ingegneria, Via Orabona 4, 70125 Bari, Italy*

ARTICLE INFO

Article history:
Received 5 February 2007
Received in revised form
10 September 2007
Accepted 12 February 2008
Available online 23 February 2008

This work is dedicated to the memory of our colleague Prof. Gaetano Liso, recently deceased.

Keywords:
Dissolution efficiency
Oxazepam
Blends/solid dispersions
Prediction
PLS regression

ABSTRACT

Quantitative structure–property relationships were developed for predicting the enhancement of dissolution rate of the model lipophilic drug Oxazepam (Oxa) from blends (BLs) with 12 structurally different carriers at three different drug/carrier weight ratios (1/5, 1/10, and 1/20). To this end, 36 BLs were prepared by the solvent-evaporation method and characterized by spectroscopic (FT-IR), thermoanalytical (DSC) and X-ray diffraction studies. The dissolution rate of the examined systems was quantified by log DE/DE_{Oxa}, where DE and DE_{Oxa} are the dissolution efficiencies of the BL and pure drug, respectively. Twenty molecular descriptors, including parameters for size, lipophilicity, cohesive energy density (CED), and hydrogen bonding capacity were calculated and together with the experimental melting point (MP), were used in multivariate analysis. Twelve pertinent variables were detected after looking at the results of principal component analysis (PCA) and cluster analysis, and reliable six-descriptor models generated by Partial Least Squares-Projection to Latent Structures (PLS) method. Satisfactory coefficient of determination values were obtained (i.e., R^2 equal to 0.794 and Q^2 equal to 0.705). The equations generated can predict with reasonable accuracy the dissolution rate increase of the model lipophilic drug/carrier BLs.

1. Introduction

The enhancement of dissolution rate and oral bioavailability of poorly water-soluble drugs represents one of the most challenging aspects in their formulation development. Among the different approaches directed at improving dissolution rate and bioavailability, the solid dispersion (SD) technology has been widely investigated (Serajuddin, 1999; Leuner and Dressmann, 2000; Craig, 2002). This technique allows a size reduction of drug particles until molecular level in a hydrophilic or amphiphilic carrier. Once the drug/carrier matrix is exposed to aqueous media, its dissolution occurs. In vivo performance of these systems depends greatly on the nature of the excipients and the method of manufacturing used. Depending on the state of the drug within the system, SDs can be classified in amorphous or crystalline (Vippagunta et al., 2007). Although the dissolution improvement may not be as significant as that with amorphous SDs, the crystalline ones are thermodynamically stable and it is a distinct advantage over the amorphous systems. Currently, the formulator has few guidelines or rules for predicting which carrier will provide the higher dissolution rate and better bioavailability of a lipophilic drug. In the last few years some advances in this regard have been made. The contributions of Rowe and co-workers (Hancock et al., 1997), as well as Barra et al. (1999) have highlighted the importance of solubility parameters and surface energy concepts for predicting excipient/excipient and drug/excipient interactions during the major processing steps of solid dosage forms. In the case of SDs, it seems plausible to relate dissolution properties and bioavailability with solubility parameters such as the Hildebrand total- and the Hansen partial (dispersion, polar, hydrogen bonding)-solubility parameters (δ_{tot} and δ_d, δ_p, δ_h, respectively). This assumption is essentially based on the transfer of the concept of "liquid regular solution" to "solid solution" where the drug powder is "dissolved" into the solid carrier. According to Fedor's report (1974), calculation of solubility parameters for both drugs and carriers can be made using the group contribution method involving molar vaporization energies and molar volume values. This methodology has been successively developed by van Kravelen, Beerbower, and Hansen and Beerbower (Hansen, 2000). Recently, some computer programs based on the group contribution procedures have became available

* Corresponding author. Tel.: +39 080 5442764. fax: +39 080 5442754.
E-mail address: trapani@farmchim.uniba.it (G. Trapani).

0378-5173/$ – see front matter © 2008 Elsevier B.V. All rights reserved.
doi:10.1016/j.ijpharm.2008.02.018

(Hansen, 2000; Breitkreutz, 1998) enabling a fast partial and total solubility parameters calculation.

The aim of the present study was to look for a correlation between theoretically computed molecular descriptors, including total and partial solubility parameters, of some carriers and the observed dissolution efficiency (DE) of the blends (BLs) containing a poorly water-soluble drug. Oxazepam (Oxa) was chosen as model drug, taking into account that a number of SDs of this lipophilic benzodiazepine compound have previously been described (Arias et al., 1998; Gines et al., 1996; Jachowicz and Nürnberg, 1997; Jachowicz et al., 1993).

2. Materials and methods

2.1. Chemicals

Oxa was extracted from tablets of Serpax® 30 (Wyeth Lederle, Aprilia, Italy) purchased from a local drugstore as follows: thirty Serpax® 30 tablets were powdered in a mortar and the powder dissolved in 10% aqueous $NaHCO_3$ (50 ml). The solution was transferred to a shake flask and extracted with ethyl ether (3 ml × 30 ml), dried (Na_2SO_4), and evaporated. Identity and purity of Oxa was checked by combining spectral data (IR, NMR and mass spectra) with elemental analysis, Gas-Chromatography (GC) and HPLC traces. Within the limits of the analytical techniques used, it is possible to state that no degradant was present in the extracted compound. Reagents used for the preparation of the buffers were of analytical grade. Polyethylene glycol 6000 (PEG 6000), polyvinylpyrrolidone (PVP) K-30, mannitol, citric acid, anhydrous lactose, urea, nicotinamide, succinic acid, sucrose, raffinose, and trehalose were purchased from Aldrich (Milan, Italy). Sorbitol was obtained from Janssen Chimica (Beerse, Belgium). Fresh deionized water was used in the preparation of the solutions. HPLC mobile phase was prepared from HPLC-grade methanol.

2.2. Apparatus

High-performance liquid chromatography (HPLC) analyses were performed using a Waters Associates Model 590 pump equipped with a Lab Instruments Micro UVis 20 variable wavelength UV detector, a 20 μl loop injection valve (Rehodyne). For analysis, a reversed phase Simmetry (25 cm × 4.6 mm; 5 μm particles) column in conjunction with a precolumn module was eluted by using mixtures of methanol and deionized water 75:25 (v:v). The flow rate of 0.8 ml min^{-1} was maintained. The column effluent was monitored continuously at 230 nm. Quantification of the compounds was carried out by measuring the peak areas in relation to those of standards chromatographed under the same conditions. The linear range for this determination was between 2.86 and 28.6 μg ml^{-1}.

2.3. Preparation of blends and physical mixtures of Oxa/carrier

BLs consisting of Oxa and the examined carrier in different weight ratios (1:5, 1:10 or 1:20, denoted as Oxa/carrier 1/5, 1/10, 1/20 BL, respectively) were prepared by the solvent-evaporation method as follows: To a solution of Oxa (50 mg) in ethanol 80 °C (30 ml) the appropriate amount of carrier was added. Next, the solvent was evaporated under reduced pressure at about 40 °C and the resulting residue, after drying under vacuum for 3 h, was stored for at least overnight in a desiccator. The samples prior to use were pulverized using a mortar and pestle and the powders were passed through a 280 μm sieve.

The above general procedure was slightly modified in the case of lactose where a mixture 1:1 (v:v) of ethanol 80%: water was used. Furthermore, in the cases of urea and nicotinamide, the above described ethanol solution was gently heated at 37 °C.

Physical mixtures (PMs) having the same weight ratios were prepared by thoroughly mixing in a mortar the appropriate amounts of Oxa and each carrier. The resulting mixtures were sieved through a 280 μm sieve and denoted as PM 1/5, 1/10, and 1/20, respectively.

2.4. Fourier transform infrared spectroscopy

Fourier transform IR spectra were obtained on a PerkinElmer 1600 FT-IR spectrometer. Samples were prepared in KBr disks (2 mg sample in 200 mg KBr). The scanning range was 450–4000 cm^{-1} and the resolution was 1 cm^{-1}. Eight scans were performed for each IR spectrum.

2.5. Thermal analysis

DSC curves were obtained by a Mettler Toledo DSC 822e Star^e 202 System equipped with a thermal analysis automatic program. Aliquots of about 5 mg of each sample were placed in an aluminium pan without pin. Conventional DSC measurements were performed by heating the sample to 250 °C at a rate of 5 °C min^{-1} under a nitrogen flow of 20 cm^3 min^{-1}. Indium (purity 100%) was used as the standard for calibrating temperature. Reproducibility was checked by running the sample in triplicate.

2.6. X-ray analysis

Powder X-ray diffraction (PXRD) patterns were recorded on a Philips PW 1830 powder X-ray diffractometer using Cu Kα radiation, a voltage of 30 kV and a current of 55 mA.

2.7. Dissolution studies

The samples used in these studies were freshly prepared and it was checked that no physical changes occurred in the period between sample preparation and dissolution tests. Dissolution experiments were carried out in triplicate with an Erweka DT dissolution test apparatus at 37 °C using the paddle method at a rotation speed of 60 rpm. Samples of each preparation equivalent to 8 mg of Oxa were added to the dissolution medium (400 ml of 0.05 M potassium phosphate buffer pH 7.4 at 37 °C). The volume of 400 ml was chosen taking into account the limit of quantification associated to the HPLC method used for Oxa determination. At appropriate time intervals, 2 ml of the mixture were withdrawn, filtered through a 0.22 μm membrane filter (Millipore®, cellulose acetate) in thermostated test tubes. Samples were withdrawn from a zone roughly midway between the surface of dissolution medium and the top of the rotating blade. The initial volume of dissolution was maintained by adding 2 ml of dissolution medium. About 1 ml of the clear filtrate was allowed to stand in a water bath at 37 °C until analyzed by HPLC. The injection volume was 20 μl. The results were analyzed with a standard calibration curve of the drug. The obtained results were means of three determinations with relative standard deviation (CV) values < 10%.

2.8. Dissolution efficiency (DE)

To characterize drug release profiles we used the DE parameter (Khan and Rhodes, 1975), defined as the area under the dissolution curve up to a certain time t, expressed as a percentage of the area of the rectangle arising from 100% dissolution in the same time. DE can be calculated by the following equation:

$$\mathrm{DE} = \int y \frac{\mathrm{d}t}{100t}$$

where y is the drug percent dissolved at time t. In this paper, all dissolution efficiencies were obtained with t equal to 180 min.

The areas under the curve (AUC) were calculated for each dissolution profile by the trapezoidal rule implemented on GraphPad Prism Version 3 for Windows software (GraphPad Software, San Diego, CA). A convenient quantification of the effect of the carrier on Oxa dissolution may be obtained by considering $\log \mathrm{DE}/\mathrm{DE}_{\mathrm{Oxa}}$, where DE and $\mathrm{DE}_{\mathrm{Oxa}}$ are the dissolution efficiencies of the BL and the pure drug, respectively.

2.9. Selection of carriers and models development

For the present study we chose a number of carriers, both polymeric and non-polymeric in nature, already used in the SD technology. In order to simplify our analysis, we ruled out gel- or self-emulsion-forming carriers. In particular, we considered the following 12 carriers: the polymers PEG 6000 and PVP K-30, the polyols mannitol and sorbitol, citric acid and succinic acid, the bases urea and nicotinamide and, finally, the sugars anhydrous lactose, sucrose, raffinose and trehalose.

The following approach was pursued to develop models able to predict $\log \mathrm{DE}/\mathrm{DE}_{\mathrm{Oxa}}$: (i) preparation by the solvent-evaporation method of BLs characterized by different drug-carrier weight ratios (1/5, 1/10, 1/20); (ii) determination of the corresponding $\log \mathrm{DE}/\mathrm{DE}_{\mathrm{Oxa}}$ values; (iii) selection of 20 potentially relevant descriptors (melting point (MP) and computed descriptors); (iv) selection of pertinent descriptors through principal component analysis (PCA) on the autoscaled matrix of the data set, combined with a cluster analysis based on correlation coefficients among variables; (v) search for a relationship between the experimentally determined $\log \mathrm{DE}/\mathrm{DE}_{\mathrm{Oxa}}$ values and the computed variables, through the Partial Least Squares-Projection to Latent Structures (PLS) method.

2.10. Molecular descriptors selection

The molecular descriptors of drug and carriers used in this study are listed in Table 1. We selected these parameters because they, as physicochemical descriptors for size, lipophilicity, cohesive energy density (CED), hydrogen bonding capacity, and surface tension, may provide insight into the molecular properties that determine dissolution of BLs/SDs. To accelerate the process of calculation, we chose to avoid using descriptors whose evaluation involves 3-D geometry optimization. Molecular weight (MW), molecular volume (MV), and molar refractivity (MR) were used as molecular size descriptors. The MP is a key index of the cohesive interactions in the solid state (Jorgensen and Duffy, 2002). As a lipophilicity measure we used the

Table 1
Molecular descriptors for Oxa and carriers studied

ID	Descriptors	Type of descriptor and/or calculation
X1	Molecular weight, MW (g/mol)	
X2	Molecular volume, MV ($Å^3$)	–[a]
X3	Melting point (MP)	The melting point data came from several sources: the Merck index, Chemfinder website, and the analytical profile of drug substances
X4	Calculated molecular refractivity (CMR)	–[b]
X5	Calculated log $P_{o/w}$ (Clog P)	–[b]
X6	Topological surface area, TPSA ($Å^2$)	Calculated by the procedure of Ertl et al. (2000)
X7	Total number of hydrogen bonds (H_{tot})	Calculated according to Ren et al. (1996)
X8	Number of oxygen and nitrogen atoms (*n*ON)	Calculated by the chemical formula
X9	Number of OH and NH groups (*n*OHNH)	Calculated by the chemical formula
X10	δ_{tot} (Total solubility parameter)	–[c]
X11	δ_d (Partial solubility parameter, dispersion component)	–[c]
X12	δ_p (Partial solubility parameter, polar component)	–[c]
X13	δ_h (Partial solubility parameter, hydrogen bonding component)	–[c]
X14	Calculated water solubility (log S_w)	–[d]
X15	Calculated pK_a	–[d]
X16	Calculated surface tension	–[a]
X17	Calculated density	–[a]
X18	Calculated $\Delta\delta_{tot}$	
X19	I_{pol}	
X20	I_{sug}	

The molecular descriptors of carriers used in this study

Carrier	MW	MV	MP	CMR	Clog P	TPSA	H_{tot}	*n*ON	*n*OHNH	δ_{tot}	δ_d	δ_p	δ_h	log *S*	pK_a	Superficial tension	Density	$\Delta\delta_{tot}$	I_{pol}	I_{sug} Pos
PEG 6000	1031	906.3	62	25.19	0.05	243.6	50	24	2	21.54	17.88	2.96	11.63	5.05	14.36	40.4	1.117	7.23	1	0
PVP K-30	794	628.4	165	21.71	−0.82	142.16	21	14	0	24.26	21.41	5.79	9.83	−2.35	−0.58	65.7	1.307	4.52	1	0
Mannitol	182.17	114.1	166	3.88	−2.05	121.37	18	6	6	39.84	19.03	10.28	33.46	0.98	14.28	99.8	1.596	−11.06	0	0
Citric acid	192.13	109	153	3.68	−1.56	132.13	18	7	4	31.38	20.92	8.24	21.89	6.76	3.85	103.9	1.762	−2.6	0	0
Lactose	342.3	193.6	200	7.07	−4.4	189.53	30	11	8	43.96	24.19	11.23	34.94	−0.36	14.48	116.4	1.8	−15.18	0	1
Urea	60.06	49.5	133	1.41	−1.66	69.12	8	3	4	35.55	19.43	21.62	20.47	1.4	14.73	55.3	1.212	−6.77	0	0
Nicotinamide	122.13	101.3	131	3.35	−0.21	55.99	6	3	2	27.23	19.96	13.11	13.08	−0.56	14.83	54.8	1.204	1.55	0	0
Succinic acid	118.1	83.8	188	2.41	−0.53	74.6	10	4	2	24.3	17.94	6.66	14.97	5.37	4.55	61.6	1.408	4.48	0	0
Sorbitol	182.17	114.1	91	3.88	−2.05	121.37	18	6	6	39.84	19.03	10.28	33.46	0.98	14.28	99.8	1.596	−11.06	0	0
Sucrose	342.3	192.8	185	7.07	−3.09	189.53	30	11	8	44.35	24.68	11.32	35.07	−0.42	14.44	113	1.77	−15.57	0	1
Raffinose	504.44	277.8	118.5	10.44	−4.66	268.68	43	16	11	41.35	23.19	8.79	33.09	−1.76	14.44	120.7	1.81	−12.57	0	1
Trehalose	342.3	193.6	98	7.07	−3.26	189.53	30	11	8	43.96	24.19	11.23	34.94	−0.45	14.48	110.8	1.76	−15.18	0	1

[a] Calculated by ACD/Labs computer program. ACD/Labs package, release 5.0 (Advanced Chemistry Development Inc., Toronto, Ontario, Canada).
[b] CLOG P for Windows Version 4.0 (BioByte Corp., Claremont, CA, USA).
[c] Calculated by the SPWin Version 2.11 computer program.
[d] ACD/Labs computer program. ACD/Labs package, release 7.0 (Advanced Chemistry Development Inc., Toronto, Ontario, Canada).

log *P* (log of octanol/water partition coefficient), which correlates well with aqueous solubility (Yalkowsky and Valvani, 1980). The commercially available ACD/Labs (ACD/Labs package, release 5.0, Advanced Chemistry Development Inc., Toronto, Ontario, Canada) and CLOG P (CLOG P for Windows Version 4.0, BioByte Corp., Claremont, CA, USA) computer programs provided us with the MV, Clog P and CMR calculations, respectively. As hydrogen bonding descriptors of a solute we used the total number of hydrogen bonds (H_{tot}), the number of oxygen and nitrogen atoms (*n*ON), and the number of OH and NH groups (*n*OHNH) (Bergström et al., 2002). However, simple count of H_{tot}, *n*ON and *n*OHNH give rise to inaccurate measure of hydrogen bonding capacity, whereas polar surface area (PSA, molecular surface area contributed by polar atoms, i.e., atoms capable of hydrogen bonding such as nitrogen and oxygen) has been found as an appropriate descriptor of hydrogen bonding capacity (Bergström et al., 2002). A simple method to evaluate PSA based solely on topological information was proposed by Ertl et al. (2000), who termed their results as topological PSA (TPSA). This protocol was used for assessing TPSA as a further hydrophilicity descriptor of the chemicals investigated.

Water solubility ($\log S_w$) and pK_a of the drug and carriers were calculated using the $\log S_w$ and pK_a (ACD/Labs) computer programs, respectively and were also included in this study.

The Hildebrand solubility parameter δ_{tot}, which is related to the CED (i.e., the cohesive energy per unit of volume) of a substance in its condensed state and the partial solubility parameters δ_d, δ_p, and δ_h, introduced by Hansen (2000) on accounting for non-polar (dispersive), polar, and hydrogen bonding effects, respectively, were calculated by employing the SPWin 2.1 program (Breitkreutz, 1998) based on the group contribution procedures. Calculated superficial tension, density (both by ACD/Labs computer program) and the difference between the total solubility parameters of drug and carrier (i.e., $\Delta\delta_{tot}$) were also included. Two indicator variables were also used to account for the presence (+1) or absence (0) of a polymeric carrier (I_{pol}) and the presence (+1) or absence (0) of a sugar carrier (I_{sug}) (Table 1).

It should be noted that the group contribution method implemented on SPWin 2.1 software package (Breitkreutz, 1998) has been actually developed for low molecular weight substances. The solubility parameter molecular descriptors for macromolecular carriers (i.e., PEG 6000 and PVP K-30) were estimated considering their mean molecular weights (6000 and 30,000 Da, respectively) and polymerization degrees. The good agreement observed between the calculated δ_{tot} and those reported in the literature for these two polymers led us to confidently assume that the involved partial values are accurate enough. Finally, the remaining descriptors for PEG 6000 and PVP K-30 were calculated by using 1031 and 794 as truncated values of the respective mean molecular weights.

2.11. Regression analysis

PCA and the partial least squares (PLS) methods were performed using the Unscrambler software (v. 7.5, CAMO ASA, Oslo, Norway). Cluster analysis was carried out using the StatGrafic Plus software (v. 5.1, Manugistics, Inc., Rockville, MD).

3. Results and discussion

The objective of this work was to look for a correlation between theoretically computed molecular descriptors of some carriers, and the observed DE of Oxa containing BLs. These systems were prepared by the solvent-evaporation method (i.e., a well established method for preparing SDs). The resulting systems were characterized at the solid-state and their dissolution behaviour was investigated.

3.1. Solid-state characterization

The purpose of these studies was to characterize the Oxa/carrier systems and to estimate the possible interaction between Oxa and a carrier in the solid state.

The FT-IR spectrum of Oxa displayed two strong absorption bands at 1713 and 1692 cm^{-1}, due to C=O and C=N stretching, respectively, and a further absorption at 3341 cm^{-1} attributable to the O–H group. In the FT-IR spectra of PEG 6000-, lactose-, and trehalose-based BLs, the absorption bands at 1713 and 1692 cm^{-1} were present, though they showed reduced intensities (data not shown). These absorption bands are absent in the FT-IR spectra of PVP-, nicotinamide-, sorbitol- and raffinose-based BLs. In these spectra, only a broad band characteristic of the pure carrier was generally detected in the 1600–1700 cm^{-1} region. This band presumably masks the drug absorption bands. In the FT-IR spectrum of mannitol-based BLs, the characteristic absorption bands of the pure carrier are present together with only a weak absorption band at 1713 cm^{-1}. Therefore, it can be concluded that no interaction between Oxa and PEG 6000-, lactose-, trehalose, or mannitol should occur, while in the remaining cases no conclusion could be drawn in this regard. In Fig. 1 the FT-IR spectra of selected carriers and BLs are shown together with that of the pure drug.

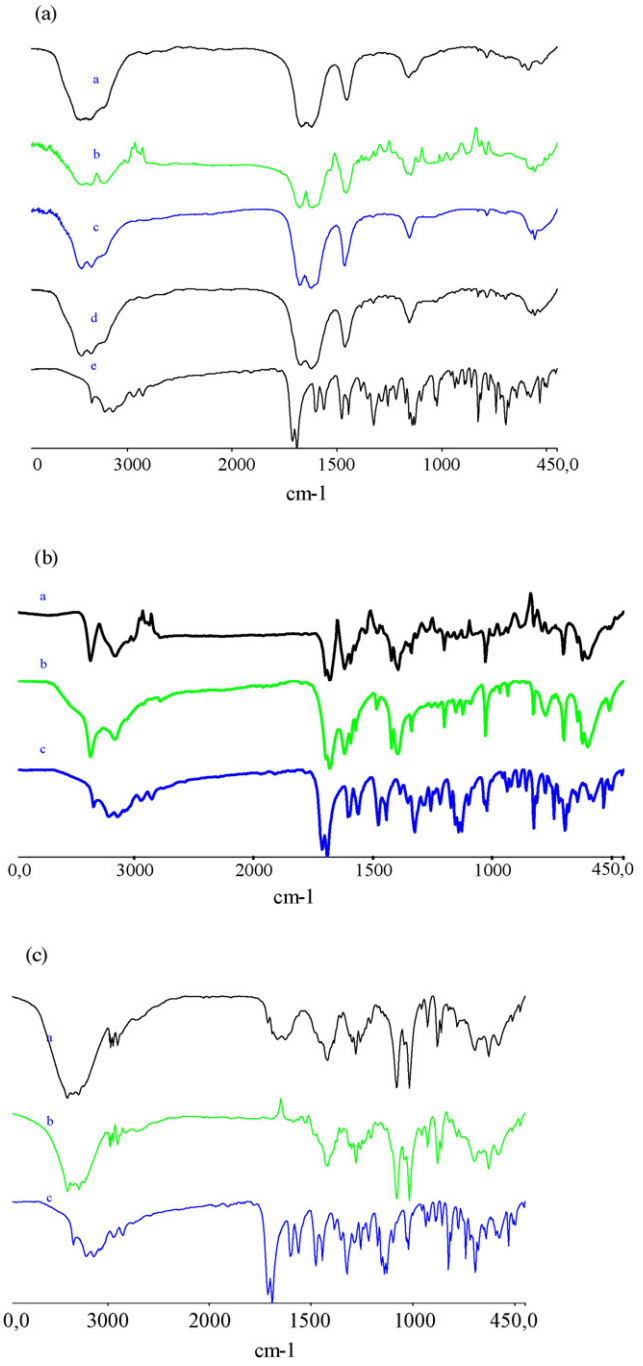

Fig. 1. FT-IR spectra of Oxa and selected BLs and carriers. (a): (a) BL Oxa/urea 1/10; (b) urea; (c) BL Oxa/urea 1/5; (d) BL Oxa/urea 1/20; (e) Oxa. (b): (a) Nicotinamide; (b) BL Oxa/nicotinamide 1/10; (c) Oxa. (c): (a) BL Oxa/mannitol 1/10; (b) mannitol; (c) Oxa.

DSC profiles of Oxa, urea, mannitol, sorbitol, nicotinamide, and selected BLs and PMs are shown in Fig. 2. The DSC curve of pure Oxa powder showed a single endothermic peak at about 197 °C, corresponding to the melting of the drug. Such a peak did not occur in the DSC curves of the BLs. The DSC profiles of the PEG-based

systems exhibited a melting endotherm at about 60 °C, while the polymer fusion was found to occur at 62 °C. Interestingly, urea- and sorbitol-based BLs and PMs show appreciable differences in their DSC thermograms, depending on the weight ratio of the drug/carrier employed (Fig. 2c and f). Furthermore, PVP-based BLs were characterized by DSC curves indicative of an amorphous physical state (Fig. 2b). PEG-, nicotinamide, and mannitol-based systems showed a little shift at lower temperatures of the endothermic peak corresponding to the melting of the carrier (Fig. 2a, d, and e, respectively).

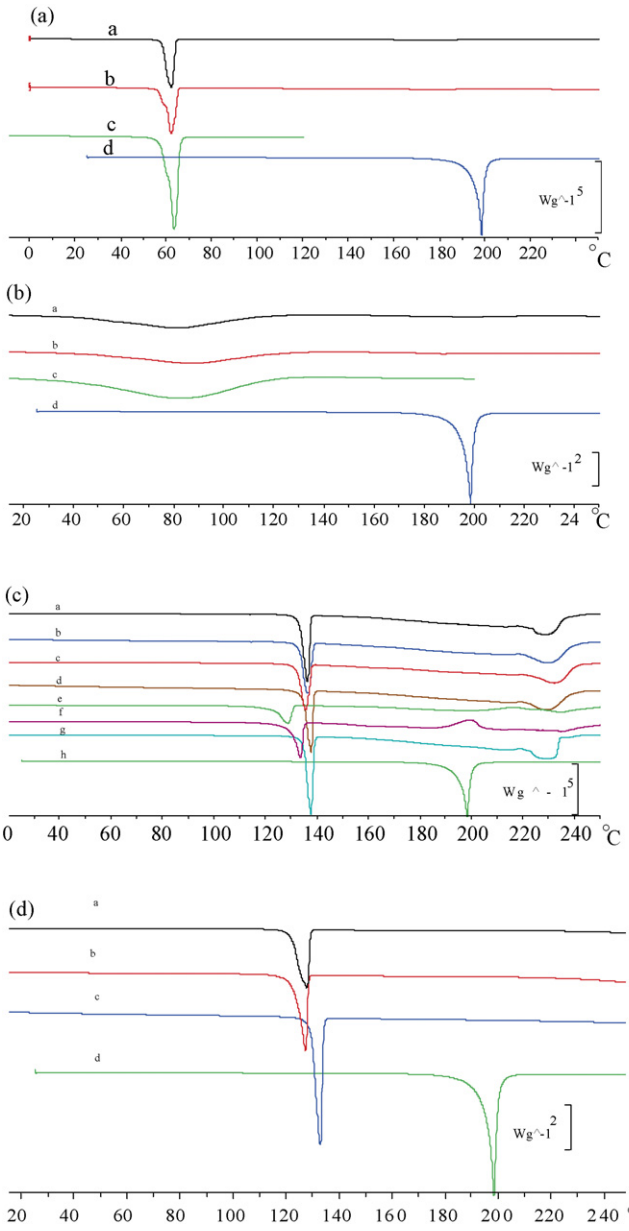

Fig. 2. DSC curves of pure drug and selected BLs, PMs, and carriers. (a): (a) PM Oxa/PEG 6000 1/10; (b) BL Oxa/PEG 6000 1/10; (c) PEG 6000; (d) Oxa. (b): (a) PM Oxa/PVP1/10; (b) BL Oxa/PVP 1/10; (c) PVP; (d) Oxa. (c): (a) PM Oxa/urea 1/20; (b) PM Oxa/urea 1/10; (c) PM Oxa/urea 1/5; (d) BL Oxa/urea 1/20; (e) BL Oxa/urea 1/10; (f) Oxa/urea 1/5; (g) urea; (h) Oxa. (d): (a) PM Oxa/nicotinamide 1/10; (b) BL Oxa/nicotinamide 1/10; (c) nicotinamide; (d) Oxa. (e): (a) PM Oxa/mannitol 1/10; (b) BL Oxa/mannitol 1/10; (c) mannitol; (d) Oxa. (f): (a) PM Oxa/sorbitol 1/20; (b) PM Oxa/sorbitol 1/10; (c) PM Oxa/sorbitol l/5; (d) BL Oxa/sorbitol 1/20; (e) BL Oxa/sorbitol 1/10; (f) BL Oxa/sorbitol 1/5; (g) sorbitol; (h) Oxa.

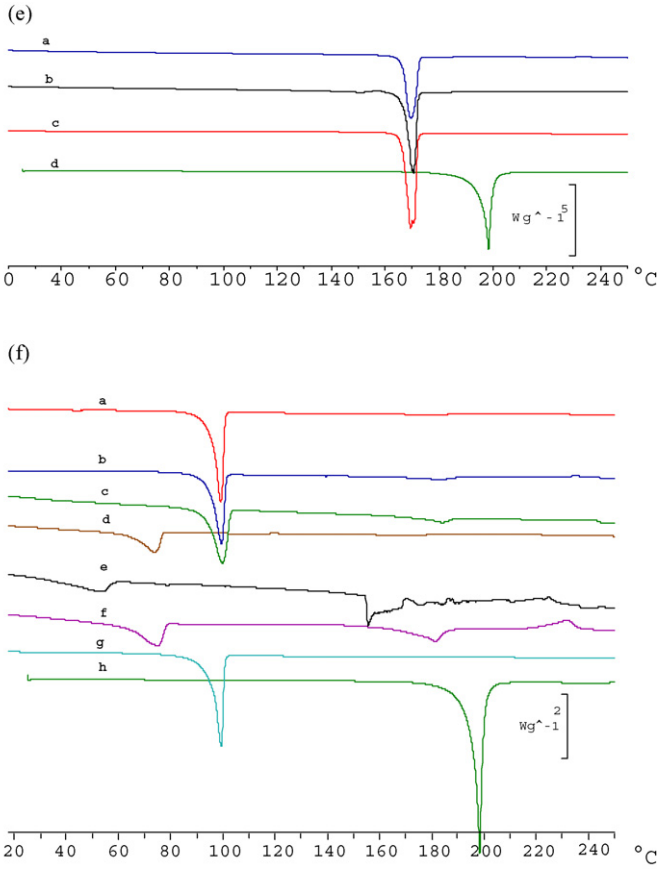

Fig. 2. (*Continued*).

These results, taken together, indicate that BL formation produces generally a marked decrease in the crystallinity of Oxa and/or it is no longer present as a crystalline material. These suggestions were further supported by the analysis of X-ray diffraction patterns of Oxa and its BLs (data not shown). In the X-ray diffraction spectra of the Oxa/carrier systems, diffraction peaks corresponding to the employed carrier were present but not the characteristic peaks of crystalline Oxa at 2ϑ 6.58°, 19.80°, and 29.43°. From these data it appears that the solid-state properties of the carrier in the examined BLs range from amorphous (e.g., PVP) to semicrystalline (e.g., PEG) to crystalline (e.g., mannitol). However, it should be taken into account that the degree of crystallinity for the Oxa/carrier systems cannot be quantified with higher accuracy and precision since it is well known that determination of low values of amorphous/crystalline phases by DSC or PXRD was proved to be ineffective (Shah et al., 2006). Finally, from the obtained data, it can be concluded that the physical structure of the BLs cannot be referred as SD in all cases but only in defined circumstances the BLs form SDs. It is a consequence of the diverse nature of the carriers investigated. Thus, it seems that Oxa/urea and Oxa/sorbitol BLs do not form SD, while systems as the PVP- and PEG-based BLs can be considered as amorphous and partially crystalline SDs, respectively.

3.2. Dissolution studies

In Fig. 3 the dissolution profiles of all BLs are also shown. The dissolution profiles were evaluated on the basis of the DE parameter up to 180 min. The results of these studies are shown in Table 2. As can be seen from the reported data, in several cases high DE values were

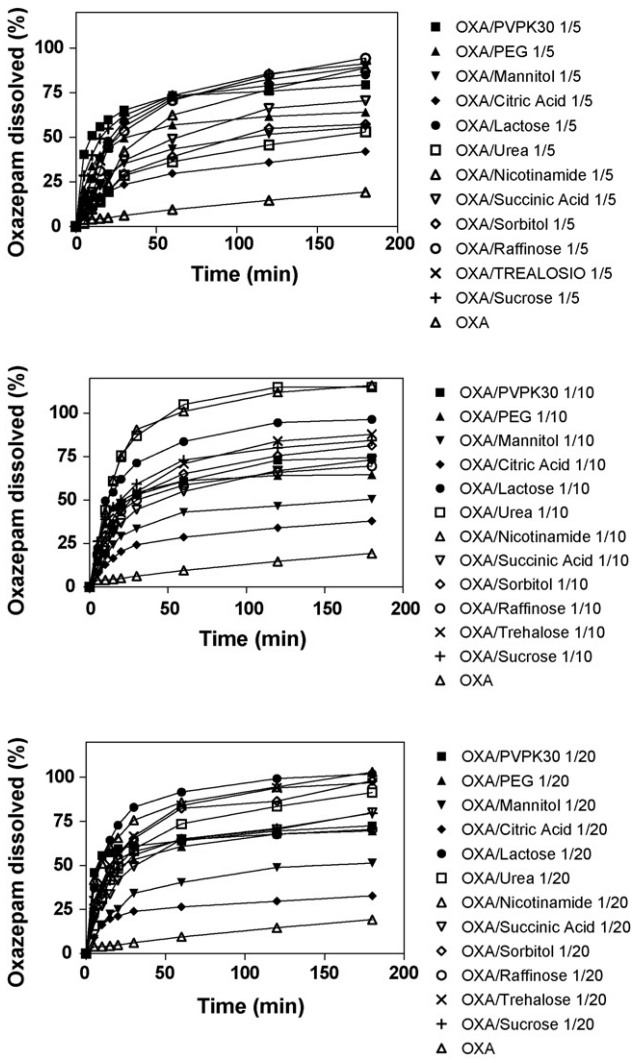

Fig. 3. Dissolution profiles in 0.05 M potassium phosphate buffer pH 7.4 at 37 °C ($n = 3$) of the BLs examined.

obtained. However, mannitol- and citric acid-BLs gave in all cases low DE values indicating that these carriers are detrimental for DE enhancement. According to literature, a decrease in crystallinity and improved wettability of the drug are considered important factors in determining the enhanced dissolution rate from SD (Van den Mooter et al., 2001). However, further mechanisms have been proposed to account for the increase in dissolution rate of drugs from their SDs. These mechanisms include carrier-controlled dissolution (Dubois and Ford, 1985; Craig and Newton, 1992; Craig, 2002), continuous drug layer formation (Dubois and Ford, 1985), and drug-controlled dissolution (Sjökvist-Saers and Craig, 1992; Craig, 2002).

3.3. Models development

Given that SD can be defined as a molecular dispersion of a drug in a hydrophilic or amphiphilic carrier (Serajuddin,1999; Leuner and Dressmann, 2000), the transfer of the concept of "liquid regular solution" to "solid solution" where the drug is "dissolved" into the solid carrier may be generally accepted. As a consequence, it would be expected that when the solubility parameter of the drug is more alike to that of the carrier, the greater should be drug dissolution rate and bioavailability. Recently, in line with these expectations, Greenhalgh et al. (1999), suggested that Hildebrand parameters give an indication of the miscibility/compatibility between drug and carrier in SD; in particular, it has been proposed that good miscibility/compatibility occurs when the calculated difference in drug/carrier total solubility parameters ($\Delta\delta = \delta_{tot}$ drug $- \delta_{tot}$ carrier) is below 7, and that complete immiscibility will result with $\Delta\delta$ values above 15. Moreover, since an increase in solubility leads to an increase in dissolution rate, a further implication of the above mentioned concept is the possibility of a relationship between solubility parameters and dissolution rate. Greenhalgh and Cook (2000) recently reported results from a preliminary study demonstrating a relationship between similarity of solubility parameters of griseofulvin and selected carriers with increased dissolution rate of the drug. Unfortunately, only the main conclusions without detailed results have been provided in this study.

It in an attempt to exploit a new approach for rationally choosing carriers in the SD technology, our initial goal was to construct models involving combinations of total-, partial-, and difference drug/carrier-solubility parameters and the data set of the dependent variable (log DE/DE_{Oxa} values). However, multiple linear regression analysis, carried out by using only total-, partial-, and difference drug/carrier-solubility parameters as independent variables yielded poor results. Next, taking into account that the number of descriptors devised is huge, a selection of pertinent predictors through PCA on the autoscaled matrix of the data set was used, combined with a cluster analysis based on correlation coefficients among variables. Autoscaling consists of variable (column of matrix) centering (i.e., the data were mean centered) followed by column standardization obtained by dividing each matrix element by the standard deviation of the corresponding column. The PCA of the autoscaled data matrix, made up of 36 rows (SDs) and 21 columns (descriptors), showed that the first three principal components accounted for about 84% of the total variance. The loading plot of the first three PCs shows that the descriptors *n*OHNH, δ_{tot}, δ_h, δ_d, superficial tension, and density are grouped in a cluster and contain similar information. Thus, looking at PCA and cluster analysis results (Fig. 4), the nine calculated predictors MW, Clog P, log S_w, density, δ_{tot}, δ_d, δ_p, TPSA and *n*ON, together with both the experimental MP, and the two indicator variables I_{pol} and I_{sug}, were selected and used in the regression calculations. There are a total of $2^n - 1$ possible combinations for a data set consisting of n descriptors. In the case under examination there are $2^{12} - 1$ combinations of descriptors. However, it is usually recommended to have at least five compounds per variable in a linear regression to produce reliable models. Hence, we considered (out of the 36 compounds) only models containing no more than six terms (descriptors) as initial input. It is well known that the partial least squares (PLS) method is particularly suited for the extraction of a few highly significant factors from large sets of correlated descriptors. Therefore, in this study, correlation between the selected descriptors and log DE/DE_{Oxa} values were established by PLS. The best PLS model on 4 principal components yielded a six-parameter equation which explains more than 60% of the log DE/DE_{Oxa} data variance (Model 1, Table 3).

A careful examination of the predicted vs. observed log DE/DE_{Oxa} (Table 2) revealed that three samples (i.e., Oxa/urea 1/5-, Oxa/urea 1/10-, and Oxa/sorbitol 1/20-BLs) behaved as strong outliers in the model derived showing high residuals (i.e., log DE/DE_{Oxa} observed – log DE/DE_{Oxa} calculated). The poor estimation of these dissolution efficiencies may be explained by taking into account the results of the corresponding X-ray diffraction patterns and thermal analyses. As mentioned above, urea- and sorbitol-containing BLs show appreciable differences in DSC thermograms (as well as in X-ray diffraction patterns) depending on the weight ratio of the drug/carrier employed. Furthermore, Oxa/sorbitol 1/20 BLs, unlike

Table 2
Observed and predicted log DE/DE_{Oxa} values for the examined BLs[a]

No.	SD	DE (%)	og DE/DE_{Oxa} observed[b]	og DE/DE_{Oxa} predicted[c] (Model 1)	og DE/DE_{Oxa} predicted[c] (Model 2)	og DE/DE_{Oxa} predicted[c,d] (Models 3–5)
1	Oxa/PEG 6000 1/5	55.44	0.674	0.731	0.732	0.754
2	Oxa/PVP 1/5	70.67	0.780	0.771	0.751	0.838
3	Oxa/mannitol 1/5	43.59	0.572	0.608	0.585	0.550
4	Oxa/citric acid 1/5	33.76	0.421	0.448	0.439	0.487
5	Oxa/lactose 1/5	71.83	0.773	0.769	0.773	0.751
6	Oxa/urea 1/5	37.86	0.510	0.785	–	0.555
7	Oxa/nicotinamide 1/5	62.55	0.727	0.808	0.830	0.700
8	Oxa/succinic acid 1/5	52.8	0.653	0.616	0.609	0.552
9	Oxa/sorbitol 1/5	42.65	0.561	0.608	0.585	0.555
10	Oxa/sucrose 1/5	74.5	0.803	0.792	0.801	0.791
11	Oxa/raffinose 1/5	71	0.782	0.780	0.761	0.791
12	Oxa/trehalose 1/5	70.5	0.779	0.795	0.802	0.792
13	Oxa/PEG 6000 1/10	58.44	0.698	0.731	0.732	0.710
14	Oxa/PVP 1/10	61.66	0.721	0.771	0.751	0.808
15	Oxa/mannitol 1/10	41.03	0.544	0.608	0.585	0.635
16	Oxa/citric acid 1/10	34.37	0.399	0.448	0.439	0.444
17	Oxa/lactose 1/10	89.5	0.847	0.769	0.773	0.755
18	Oxa/urea 1/10	99	0.930	0.785	–	0.931
19	Oxa/nicotinamide 1/10	98.67	0.925	0.808	0.830	0.899
20	Oxa/succinic acid 1/10	56.4	0.682	0.616	0.609	0.607
21	Oxa/sorbitol 1/10	62.6	0.746	0.608	0.585	0.635
22	Oxa/sucrose 1/10	70.7	0.781	0.792	0.801	0.789
23	Oxa/raffinose 1/10	60	0.693	0.780	0.761	0.742
24	Oxa/trehalose 1/10	70.3	0.778	0.795	0.802	0.788
25	Oxa/PEG 6000 1/20	60.44	0.712	0.731	0.732	0.726
26	Oxa/PVP 1/20	65	0.744	0.771	0.751	0.847
27	Oxa/mannitol 1/20	41.16	0.545	0.608	0.585	0.665
28	Oxa/citric acid 1/20	26.83	0.359	0.448	0.439	0.449
29	Oxa/lactose 1/20	89.34	0.883	0.769	0.773	0.771
30	Oxa/urea 1/20	70.67	0.792	0.785	0.851	0.790
31	Oxa/nicotinamide 1/20	85.03	0.863	0.808	0.830	0.843
32	Oxa/succinic acid 1/20	62.5	0.727	0.616	0.609	0.618
33	Oxa/sorbitol 1/20	78.2	0.824	0.608	–	0.665
34	Oxa/sucrose 1/20	64.2	0.739	0.792	0.801	0.784
35	Oxa/raffinose 1/20	62.1	0.724	0.780	0.761	0.806
36	Oxa/trehalose 1/20	81.5	0.842	0.795	0.802	0.847

[a] DE Oxa was found equal to 11.7%.
[b] Observed experimental dissolution efficiency enhancement.
[c] Calculated dissolution efficiency enhancement.
[d] Model 3 for blendss 1/5; Model 4 for blendss 1/10; Model 5 for blendss 1/20.

the corresponding 1/5 and 1/10 systems, has the composition of a thick glassy gel. On the other hand, it is possible that in the case of urea and with particular drug loading, formation of systems as clathrates or channel-like complexes, very different from SD, occurs (Martin, 1993). All these observations induce us to believe that a different mechanism of dissolution is involved for these outliers. By removing the outliers mentioned above, a better PLS model with satisfactory statistics was again obtained (Model 2, Table 3). With the same independent variables of Model 2 applied to the BLs 1/5 or 1/10 or 1/20, respectively, significant results were obtained for 1/5 or 1/10 or 1/20 BLs (Models 3–5, Table 3). However, the predictive ability of Models 3 and 4 is good, while that of Model 5 is poor. It should be noted that Model 2, (i.e., the model derived from a set of BLs essentially constituted by SDs) may represent a quantitative

Table 3
Predictive power of the devised PLS models[a]

Descriptors	Model 1	Model 2	Model 3 BL1/5[b]	Model 4 BL1/10[c]	Model 5 BL1/20[d]
log S_w	−0.0158	−0.0110	−0.0187	−0.0193	−0.0266
Density	−0.396	−0.485	−0.270	−0.449	−0.344
δ_d	−0.0006	0.00439	0.0142	0.00578	−0.00304
I_{sug}	0.240	0.260	0.207	0.173	0.160
Clog P	0.00749	0.00731	0.0171	0.0117	0.00197
δp	0.00254	0.00696	−0.0110	0.0109	0.000412
Intercept	1.256	1.426	0.884	1.172	1.298
Samples	36	33	12	12	12
R^2	0.609	0.794	0.840	0.806	0.602
Q^2	0.424	0.705	0.840	0.633	0.107
N_{PC}	4	4	3	3	3

[a] R^2 is the coefficient of determination, Q^2 (an assessment of the 'internal' predictive ability of the model), is the cross validated coefficient of determination. N_{PC} is the number of principal components.
[b] PLS model applied to blends 1/5.
[c] PLS model applied to blends 1/10.
[d] PLS model applied to blends 1/20.

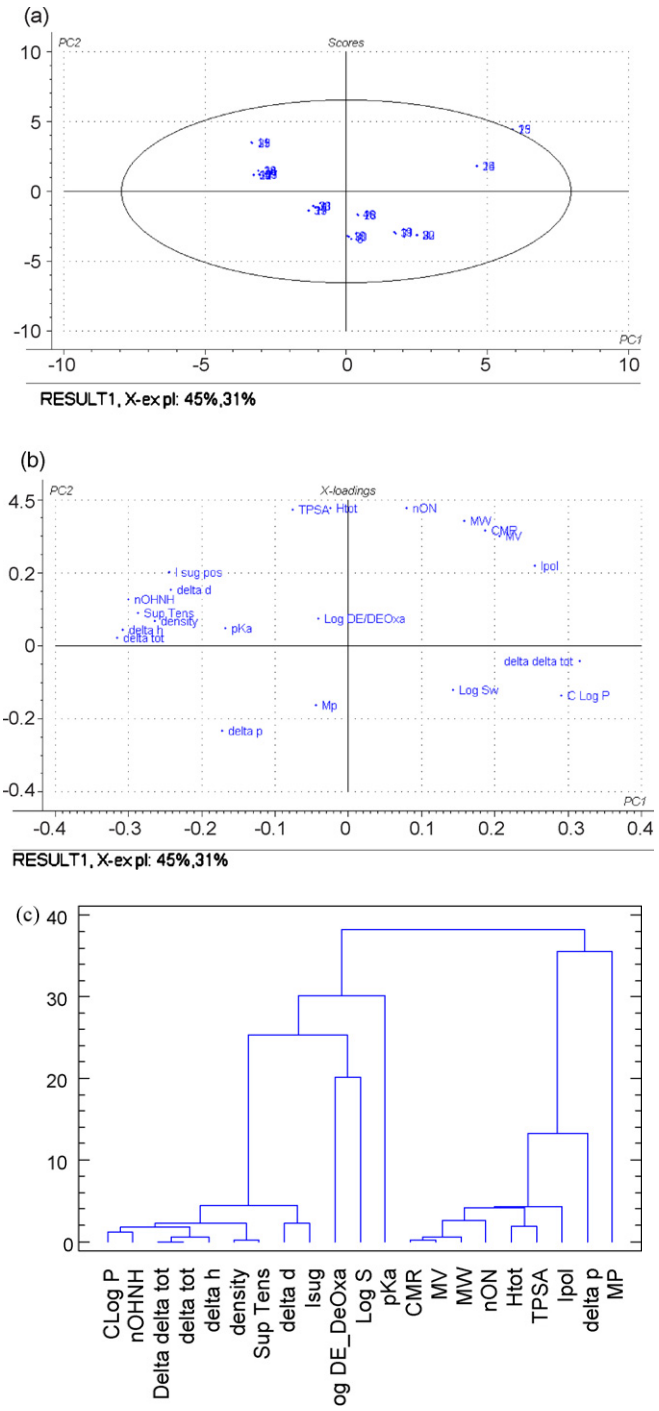

Fig. 4. (a) Heterogeneity of the dataset investigated by principal component analysis (PCA). The dataset covered all four quadrants of the PCA score plot, showing that the selected series of samples was heterogeneous; (b) loading plot showing the interrelationship between the independent variables in the description of log DE/DE_{Oxa} and (c) dendrogram of similarity among variables obtained using a hierarchical cluster analysis (nearest neighbor method, euclidean distance) based on correlation coefficients (R^2).

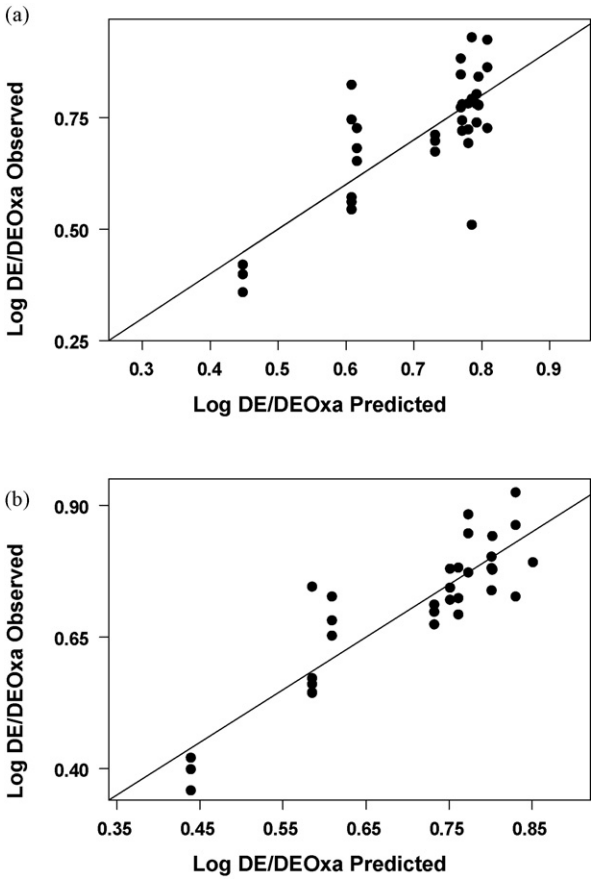

Fig. 5. Relationship between observed vs. predicted log DE/DE_{Oxa} according to (a) Model 1 and (b) Model 2.

structure–property relationship useful for predicting the enhancement of dissolution rate of the model lipophilic drug Oxa from SD forming systems.

According to the PLS analyses, the negative correlation between log DE/DE_{Oxa} and log S_w and density, indicates that the higher the carrier aqueous solubility or density, the lower the dissolution rate of the dispersion. These results may be interpreted assuming that the rate of release is controlled by that of the carrier and is independent of drug properties (i.e., carrier-controlled model), and involves the release of intact particles with dissolution occurring from a surface layer rich in one component (i.e., the carrier) (Craig, 2002). This seems a reasonable assumption taking into account that the highest drug loading examined corresponds to about 20% (i.e., 1/5 SD). Under these circumstances, taking into account that in the BLs/SDs the drug can be dispersed in the carrier also as particles (Craig, 2002), it is clear that if the water-soluble carrier dissolved more rapidly than drug, it can prevent further dissolution of drug particles from BL/SDs. On the other hand, high-density carriers can bring about drug segregation, adversely affecting its dissolution properties. Also, the role of lipophilicity descriptor (Clog P) occurring in PLS regression can be reasonably interpreted on the basis of the aforementioned model. Indeed, it is well known that lipophilicity is negatively correlated with aqueous solubility (Yalkowsky and Valvani, 1980), accounting for its positive influence on drug dissolution rate. With regard to the variable effects of the partial solubility parameters δ_d and δ_p, it seems that the carrier should possess an appropriate balance between non-polar (dispersive) and polar interactions for improving the dissolution rate of BLs/SDS. Another important point which emerges from Models 1–5 is both the positive and high value associated to the coefficient of I_{sug}. According to the PLS analyses, indeed, I_{sug} is the most important descriptor influencing the log DE/DE_{Oxa}. In Table 2, experimental and calculated log DE/DE_{Oxa} are reported. In addition, Fig. 5 presents the relationship between observed vs. predicted log DE/DE_{Oxa} by Models 1 and 2.

4. Conclusions

In the present work, rapidly available and physically meaningful descriptors of a number of commonly employed carriers were related to the log DE/DE_{Oxa} by PLS regression. Statistical criteria were used to models that combine simplicity, goodness of fit, and predictivity. This study demonstrates that, under the examined conditions (very probably involving carrier-controlled dissolution mechanisms), log DE/DE_{Oxa} cannot be modeled neither in terms of calculated superficial tension nor in terms of difference between drug/carrier total solubility parameters. The computational models developed in this study can predict the log DE/DE_{Oxa} with a reasonable degree of accuracy by using calculated carrier aqueous solubility, density, lipophilicity, the partial solubility parameters δ_d and $\delta_{p,}$ and an indicator variable accounting for the presence or absence of a sugar carrier. These models work quite well but validation with other lipophilic drugs is needed to demonstrate their general legitimacy. The appropriate use of the models generated involves at first log DE/DE_{drug} estimation provided by a given carrier (by PLS Models 1 or 2), and then identification of which weight ratio (1:5, 1:10) (by Models 3 and 4) could be more useful. While this finding deserves further investigation, the results reported herein may be of significance in the rational design of BL/SD formulations.

Acknowledgment

We thank Dr. Jörg Breitkreutz (Westphalien Wilhelms University, Münster, Germany) for having provided us with the SPWin, v. 2.1 software.

References

Arias, M.J., Moyano, J.R., Gines, J.M., 1998. Study by DSC and HSM of the oxazepam-PEG 6000 and oxazepam-D-mannitol systems: application to the preparation of SDs. Thermochim. Acta 321, 33–41.

Barra, J., Bustamante, P., Doelker, E., 1999. Use of the solubility parameter and surface energy concepts in the formulation of solid dosage forms. STP Pharma Sci. 9, 293–305.

Bergström, C.A.S., Norinder, U., Luthman, K., Artursson, P., 2002. Experimental and computational screening models for prediction of aqueous drug solubility. Pharm. Res. 19, 182–188.

Breitkreutz, J., 1998. Prediction of intestinal drug absorption properties by three-dimensional solubility parameters. Pharm. Res. 15, 1370–1375.

Craig, D.Q.M., 2002. The mechanisms of drug release from solid dispersions in water-soluble polymers. Int. J. Pharm. 231, 131–144.

Craig, D.Q.M., Newton, J.M., 1992. The dissolution of nortriptyline HCl from polyethylene glycol solid dispersions. Int. J. Pharm. 78, 175–182.

Dubois, J.L., Ford, J.L., 1985. Similarities in the release rates of different drugs from polyethylene glycol 6000 dispersions. J. Pharm. Pharmacol. 37, 494–495.

Ertl, P., Rohde, B., Selzer, P., 2000. Fast calculation of molecular polar surface area as a sum of fragment-based contributions and its application to the prediction of drug transport properties. J. Med. Chem. 43, 3714–3717.

Fedors, R.F., 1974. A method for estimating both the solubility parameters and molar volumes of liquids. Polym. Eng. Sci. 14, 147–154.

Gines, J.M., Arias, M.J., Moyano, J.R., Sanchez-Soto, P.J., 1996. Thermal investigation of crystallization of polyethylene glycols in SDs containing oxazepam. Int. J. Pharm. 143, 247–253.

Greenhalgh, D.J., Williams, A.C., Timmins, P., York, P., 1999. Solubility parameters as predictors of miscibility in SDs. J. Pharm. Sci. 88, 1182–1190.

Greenhalgh, D.J., Cook, W., 2000. Relationship between drug and carrier solubility parameters and dissolution of SD systems. J. Pharm. Pharmacol. 52, 299.

Hancock, B.C., York, P., Rowe, R.C., 1997. The use of solubility parameters in pharmaceutical dosage form design. Int. J. Pharm. 148, 1–21.

Hansen, C.M., 2000. Hansen Solubility Parameters––A User's Handbook. CRC Press, Boca Raton.

Jachowicz, R., Nürnberg, E., 1997. Enhanced release of oxazepam from tablets containing SDs. Int. J. Pharm. 159, 149–158.

Jachowicz, R., Nürnberg, E., Hoppe, R., 1993. SDs of oxazepam. Int. J. Pharm. 99, 321–325.

Jorgensen, W.L., Duffy, E.M., 2002. Prediction of drug solubility from structure. Adv. Drug Deliv. Rev. 54, 355–366.

Khan, C.A., Rhodes, C.T., 1975. The concept of dissolution efficiency. J. Pharm. Pharmacol. 27, 48–49.

Leuner, C., Dressmann, J., 2000. Improving drug solubility for oral delivery using SDs. Eur. J. Pharm.Biopharm. 50, 47–60.

Martin, A., 1993. Physical Pharmacy, fourth ed. Lea and Febiger Media, Pennsylvania, pp. 257–259.

Ren, S., Das, A., Lien, E.J., 1996. QSAR analysis of membrane permeability to organic compounds. J Drug Target 4, 103–107.

Serajuddin, A.T.M., 1999. SD of poorly water-soluble drugs: early promises, subsequent problems, and recent breakthroughs. J. Pharm. Sci. 88, 1058–1066.

Shah, B., Kakumanu, V.K., Bansal, A.K., 2006. Analytical techniques for quantification of amorphous/crystalline phases in pharmaceutical solids. J. Pharm. Sci. 95, 1641–1665.

Sjökvist-Saers, E., Craig, D.Q.M., 1992. An investigation into the mechanisms of dissolution of alkyl *p*-aminobenzoates from polyethylene glycol solid dispersions. Int. J. Pharm. 83, 211–219.

Van den Mooter, G., Wuyts, M., Blaton, N., Busson, R., Grobet, P., Augustijns, P., Kinget, R., 2001. Physical stabilisation of amorphous ketoconazole in SDs with polyvinylpyrrolidone K25. Eur. J. Pharm. Biopharm. 12, 261–269.

Vippagunta, S.R., Wang, Z., Hornung, S., Krill, S.R., 2007. Factors affecting the formation of eutectic solid dispersions and their dissolution behaviour. J. Pharm. Sci. 96, 294–304.

Yalkowsky, S.H., Valvani, S.C., 1980. Solubility and partitioning I: Solubility of nonelectrolytes in water. J. Pharm. Sci. 69, 912–922.